International Journal of Modern Physics E

Measurements of open charm hadrons in Au+Au collisions at $\sqrt{s_{\mathrm{NN}}} = 200$ GeV by the STAR experiment

Jan Vanek *for the STAR Collaboration*

Nuclear Physics Institute, Czech Academy of Sciences
Rez, Czech Republic
vanek@ujf.cas.cz

Received Day Month Year
Revised Day Month Year

At RHIC energies, charm quarks are primarily produced in hard partonic scatterings at early stages of ultra-relativistic heavy-ion collisions. This makes them an ideal probe of the Quark-Gluon Plasma (QGP), as they experience the entire evolution of this hot and dense medium. STAR is able to measure the production of charm quarks and their interaction with the QGP through direct reconstruction of hadronic decays of $\mathrm{D}^{\pm}$, D^{0}, $\mathrm{D_s}$, and $\Lambda_{\mathrm{c}}^{\pm}$ hadrons, enabled by the excellent track pointing resolution provided by the Heavy Flavor Tracker.

In these proceedings, we present the most recent results on open charm hadron production in Au+Au collisions at $\sqrt{s_{\mathrm{NN}}} = 200\,\mathrm{GeV}$ from the STAR experiment. In particular, we discuss the nuclear modification factors of $\mathrm{D}^{\pm}$ and D^{0} mesons which provide information on the charm quark energy loss in the QGP. We also present the $\mathrm{D_s}/\mathrm{D}^{0}$ and $\Lambda_{\mathrm{c}}^{\pm}/\mathrm{D}^{0}$ yield ratios as functions of transverse momentum and collision centrality which help us better understand the charm quark hadronization process in heavy-ion collisions. The spectra of D^{0}, $\mathrm{D}^{\pm}$, $\mathrm{D_s}$, and $\Lambda_{\mathrm{c}}^{\pm}$ in 10-40% central Au+Au collisions are used to calculate the total charm quark production cross section in Au+Au collisions which, compared to the charm quark cross section in p+p collisions, gives insight into charm quark production in heavy-ion collisions.

Keywords: Quark-Gluon Plasma; open-charm hadrons; STAR Experiment.

PACS numbers:

1. Introduction

The STAR experiment is a versatile experimental facility located at Brookhaven National Laboratory and is the only running experiment at the Relativistic Heavy-Ion Collider (RHIC). One of the main goals of STAR's physics program is to study the properties of an extreme state of matter in which the quarks and gluons are no longer bound inside hadrons - the Quark-Gluon Plasma (QGP). The QGP can be created in ultra-relativistic heavy-ion collisions, as supported by previous measurements from RHIC and the Large Hadron Collider (LHC) at CERN.

An example of such measurements is presented in Fig. 1 which shows the nuclear modification factor (R_{AA}) as a function of transverse momentum (p_{T}) for various

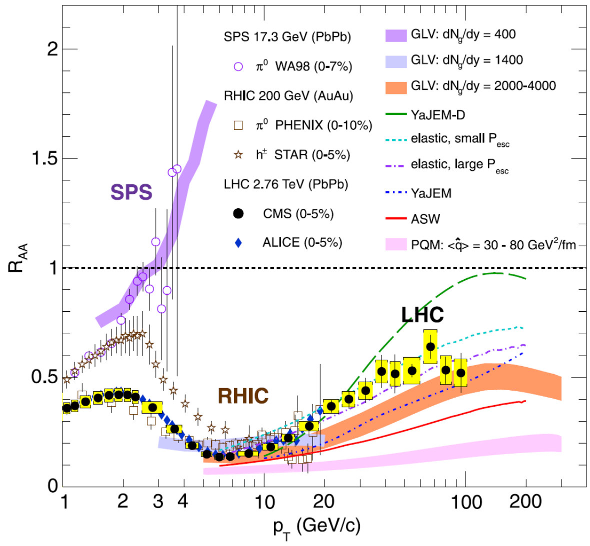

Fig. 1. Nuclear modification factor for different particle species. Shown are results from measurements of π^0 mesons in Pb+Pb collisions by the WA98 experiment[1,2] and in Au+Au collisions by PHENIX,[3] as well as charged hadrons in Au+Au collisions by STAR,[4] and in Pb+Pb collisions by the ALICE[5] and CMS[6] experiments. The collision energies are indicated in the legend. The measured data are compared to variety of model calculations.[7–12] Figure taken from Ref. 6.

particles. The $R_{\rm AA}$ is defined as:

$$R_{\rm AA} = \frac{({\rm d}N/{\rm d}p_{\rm T})_{\rm AA}}{\langle N_{\rm coll}\rangle ({\rm d}N/{\rm d}p_{\rm T})_{\rm pp}}, \qquad (1)$$

where $\langle N_{\rm coll}\rangle$ is the mean number of binary collisions and $({\rm d}N/{\rm d}p_{\rm T})_{\rm AA}$ and $({\rm d}N/{\rm d}p_{\rm T})_{\rm pp}$ are measured invariant yields of given particle species in heavy-ion collisions and p+p collisions, respectively. The $R_{\rm AA}$ is defined so that if heavy-ion collisions were just a simple superposition of p+p collisions, the $R_{\rm AA}$ would be equal to unity. This is clearly not the case for π^0 mesons and charged particles, as shown in Fig. 1. The invariant spectra of the aforementioned particles are significantly suppressed in heavy-ion collisions compared to that in the p+p collisions, which can be explained by the energy loss of partons in the QGP.

The measurements described above are dominated by light-flavor hadrons which can generally originate from the hard partonic scattering, i.e. from very early stage of the heavy-ion collision, but at low $p_{\rm T}$ also from hadronization of the QGP bulk. It is difficult to distinguish experimentally from which source a given light flavor hadron comes from. The situation is different for heavy flavor quarks, charm and bottom, which are produced dominantly in hard partonic scatterings, before the formation of the QGP. This means that they experience the whole evolution of the medium, as illustrated in Fig. 2, which makes them an ideal probe of the QGP

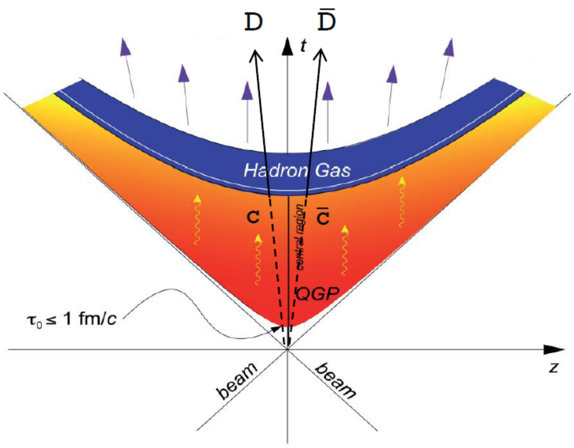

Fig. 2. Time evolution of a heavy-ion collision in the z-t plane. Taken from Ref. 13 and modified.

properties.

One convenient way to access the information about heavy-quark production is via reconstruction of open-heavy flavor hadrons. In these proceedings, we present a summary of recent results from the measurements of open-charm hadron production in Au+Au collisions at $\sqrt{s_{\mathrm{NN}}} = 200\,\mathrm{GeV}$ by the STAR experiment. The following section provides a brief overview of methods used for reconstruction of open-charm hadrons and summarizes the latest results by STAR.

2. Open-charm hadrons at STAR

At STAR, the open-charm hadrons produced in Au+Au collisions at $\sqrt{s_{\mathrm{NN}}} = 200\,\mathrm{GeV}$ are reconstructed topologically through their hadronic decays. This method is possible thanks to the excellent vertex resolution enabled by the STAR's Heavy Flavor Tracker (HFT),[14] which is a 4-layer silicon detector that was a part of the STAR detector from the year 2014 to 2016. The HFT allowed STAR to measure invariant yields of four ground states of the open-charm hadrons: D^0, $\mathrm{D}^{\pm}$, $\mathrm{D}_{\mathrm{s}}^{\pm}$ mesons, and Λ_{c} baryons.

The decay channels used for the reconstruction of the aforementioned open-charm hadrons are summarized in Tab. 1. These decay channels were chosen, as their decay topology can be easily identified utilizing the HFT and at the same time, they have relatively large branching ratios (BR). The topological selection criteria were optimized using supervised machine learning techniques implemented in the ROOT TMVA (Toolkit for Multivariate Analysis) package[15] in order to maximize the signal significance. The invariant yields of open-charm hadrons were extracted as a function of p_{T} and collision centrality. More details about the reconstruction of individual hadrons can be found in Refs. 17–19.

The measured invariant yield of D^0 mesons is used to calculate the R_{AA}. Figure 3

Table 1. List of open-charm hadrons measured at STAR using the HFT. The left column contains decay channels used for reconstruction, $c\tau$ is the mean lifetime of a given hadron, and BR is the branching ratio. Charge conjugate particles are measured as well. Values are taken from Ref. 16.

Decay channel	$c\tau$ [μm]	BR [%]
$D^0 \rightarrow K^-\pi^+$	122.9 ± 0.4	3.89 ± 0.04
$D^+ \rightarrow K^-\pi^+\pi^+$	311.8 ± 2.1	8.98 ± 0.28
$D_s^+ \rightarrow \phi\pi^+ \rightarrow K^-K^+\pi^+$	151.2 ± 1.2	2.27 ± 0.08
$\Lambda_c^+ \rightarrow K^-\pi^+p$	59.9 ± 1.8	6.35 ± 0.33

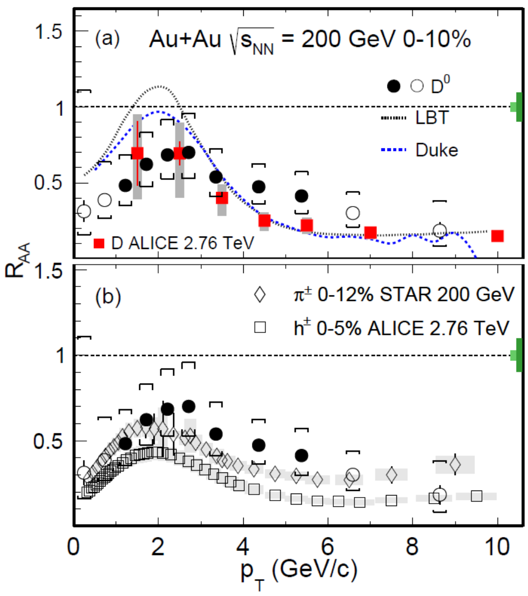

Fig. 3. Nuclear modification factor of D^0 mesons as a function of p_T measured in 0-10% central Au+Au collisions at $\sqrt{s_{NN}} = 200\,\text{GeV}$ by the STAR experiment. The data are compared to two model calculations,[21,22] to measurement of $\pi^{\pm}$ mesons in central Au+Au collisions at the same energy by STAR,[23] and to measurements of charged hadrons[24] and D mesons[25] in Pb+Pb collisions at $\sqrt{s_{NN}} = 2.76\,\text{TeV}$ by ALICE. The STAR D^0 p+p reference is taken from Ref. 26. Figure taken from Ref. 17.

shows the D^0 meson R_{AA} as a function of p_T in central Au+Au collisions at $\sqrt{s_{NN}} = 200\,\text{GeV}$. The suppression of the high-p_T D^0 mesons is similar to that of $\pi^{\pm}$ mesons in Au+Au collisions at the same energy[23] which suggests that the charm quarks loose a significant fraction of their initial energies inside the QGP medium. The data are also compared to two model calculations[21,22] and to measurements of charged hadrons and D mesons in central Pb+Pb collisions at $\sqrt{s_{\rm NN}} = 2.76\,\text{TeV}$ by ALICE.[24,25] Despite very different collision energies, the suppression of D mesons appears to be very similar at RHIC and the LHC.

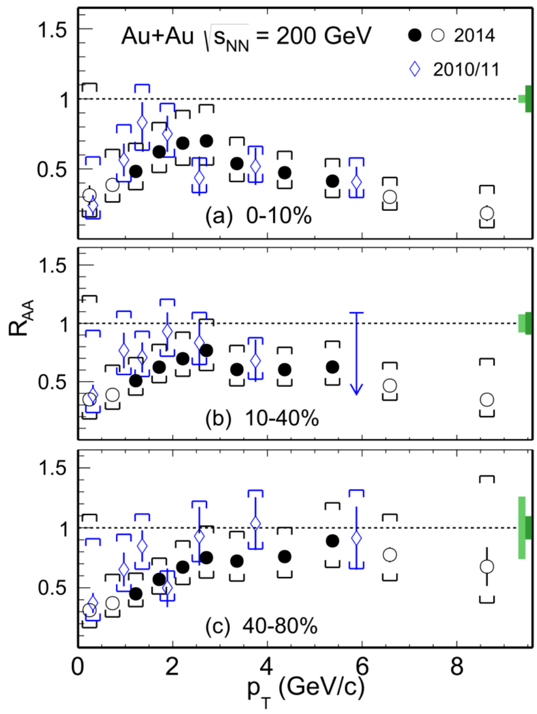

Fig. 4. $R_{\rm AA}$ of $\rm D^0$ mesons as a function of $p_{\rm T}$ measured in 0-10% (a), 10-40% (b), and 40-80% (c) central Au+Au collisions at $\sqrt{s_{\rm NN}} = 200\,\text{GeV}$ by the STAR experiment utilizing the HFT (2014)[17] and without the HFT (2010/11).[27] The p+p reference is taken from Ref. 26. Figure taken from Ref. 17.

It is also interesting to investigate the centrality dependence of the $\rm D^0$ meson $R_{\rm AA}$ which is shown in Fig. 4. In the region of $p_{\rm T} > 3\,\text{GeV}/c$, the suppression gets weaker when going from central to peripheral collisions, again supporting that the suppression is caused by energy loss of the charm quarks inside the QGP. For $p_{\rm T} < 3\,\text{GeV}/c$, on the other hand, the suppression does not depend on the centrality and is significant in all three studied centrality classes. As will be discussed later, this observation is important for understanding the charm quark hadronization in heavy-ion collisions.

The same dependence of the suppression on collision centrality is observed for $\rm D^{\pm}$ mesons, as can be seen in Fig. 5, which shows the $R_{\rm AA}$ (top) and $(\rm D^+ + D^-)/(D^0 + \bar{D}^0)$ yield ratio (bottom) as a function of $p_{\rm T}$ measured in 0-10% and

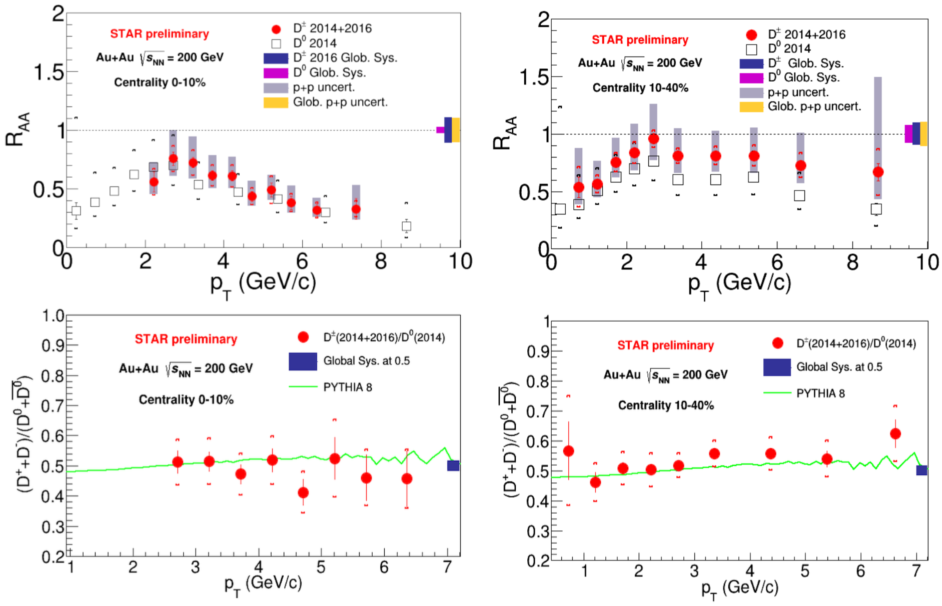

Fig. 5. R_{AA} (top) and $(\mathrm{D}^+ + \mathrm{D}^-)/(\mathrm{D}^0 + \bar{\mathrm{D}}^0)$ yield ratio (bottom) as a function of p_{T} measured in 0-10% and 10-40% central Au+Au collisions at $\sqrt{s_{\mathrm{NN}}} = 200\,\mathrm{GeV}$ by the STAR experiment. The p+p reference for the R_{AA} is taken from Ref. 26 and the D^0 meson yields in Au+Au collisions for the yield ratios are taken from Ref. 17. The yield ratios are in a good agreement with PYTHIA 8 calculation.[28]

10-40% central Au+Au collisions at $\sqrt{s_{\mathrm{NN}}} = 200\,\mathrm{GeV}$. The suppression of $\mathrm{D}^{\pm}$ and D^0 mesons is consistent within the uncertainties and their yield ratio measured in Au+Au collisions is consistent with that from PYTHIA 8 calculation. This suggests that the suppression mechanism for both D^0 and $\mathrm{D}^{\pm}$ mesons is the same.

The suppression of the p_{T}-integrated yields of D^0 and $\mathrm{D}^{\pm}$ mesons is observed in all studied centralities, which is not expected from a simple scaling of charm quark production in p+p collisions with the number of binary collisions. This is not expected from a simple scaling of charm quark production in Au+Au collisions with number-of-binary collisions. Therefore, STAR has further investigated the total charm quark production cross section in Au+Au collisions by measuring production yields of other open-charm hadron species, namely Λ_{c} baryons and $\mathrm{D}_{\mathrm{s}}^{\pm}$ mesons. Figure 6 shows the $(\Lambda_{\mathrm{c}}^+ + \Lambda_{\mathrm{c}}^-)/(\mathrm{D}^0 + \bar{\mathrm{D}}^0)$ yield ratio as a function of N_{part} (i.e. collision centrality) measured in Au+Au collisions at $\sqrt{s_{\mathrm{NN}}} = 200\,\mathrm{GeV}$.[18] The data show an enhancement of Λ_{c} baryons in central Au+Au collisions with respect to PYTHIA 8, both without (green triangle) and with (pink triangle) color re-connection (CR). The centrality dependence of the yield ratio is well described by the Catania model incorporating coalescence and fragmentation hadronization of charm quarks.[29]

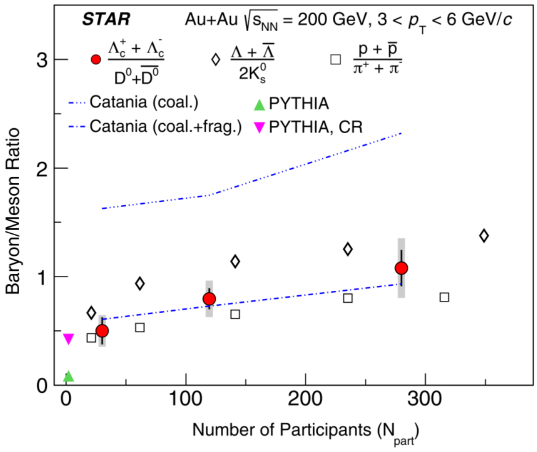

Fig. 6. The $(\Lambda_c^+ + \Lambda_c^-)/(\mathrm{D}^0 + \bar{\mathrm{D}}^0)$ yield ratio as a function of N_{part} measured in Au+Au collisions at $\sqrt{s_{\mathrm{NN}}} = 200\,\mathrm{GeV}$ by the STAR experiment. The data are compared to Catania model calculations[29] and to PYTHIA calculations with (pink triangle) and without (green triangle) color reconnection (CR). Measurements of baryon-to-meson ratios for strange[30] and light-flavor[31] hadrons are shown for comparison. Figure taken from Ref. 18.

The enhancement with respect to PYTHIA is also observed in p_{T} dependence of the $(\Lambda_c^+ + \Lambda_c^-)/(\mathrm{D}^0 + \bar{\mathrm{D}}^0)$ yield ratio, which is shown in Fig. 7. The observed ratio shows similar dependence and magnitude as baryon-to-meson ratios of strange[30] and light flavor hadrons.[31] The lower panel shows comparisons to model calculations. The enhancement increases towards lower p_{T}, which is again reasonably well described by the Catania model incorporating coalescence and fragmentation hadronization of charm quarks.[29] The data, with support of the models, suggest that coalescence hadronization of charm quarks inside the QGP plays a significant role in Au+Au collisions at $\sqrt{s_{\mathrm{NN}}} = 200\,\mathrm{GeV}$ and has profound impacts on ratios of the open-charm hadron species.

This observation is further supported by the measurement of the $(\mathrm{D}_s^+ + \mathrm{D}_s^-)/(\mathrm{D}^0 + \bar{\mathrm{D}}^0)$ yield ratio as a function of p_{T} and collision centrality,[19] as shown in Fig. 8. Similar to the Λ_c baryon, the $\mathrm{D}_s^\pm$ meson yields are enhanced with respect to the PYTHIA baseline. The observed enhancement is again consistent with significant contribution of coalescence hadronization of charm quarks inside the QGP.

At this point, the obvious question to ask is, whether the observed enhancements of Λ_c baryons and $\mathrm{D}_s^\pm$ mesons can compensate the suppression of D^0 and $\mathrm{D}^\pm$ mesons. This is checked by calculating the total production cross section of the individual open-charm hadrons, which can be then used to calculate the total charm quark production cross section in Au+Au collisions at $\sqrt{s_{\mathrm{NN}}} = 200\,\mathrm{GeV}$, as summarized in Tab. 2. The measured cross section in 10-40% central Au+Au collisions is consistent with that measured in p+p collisions at $\sqrt{s} = 200\,\mathrm{GeV}$ within the

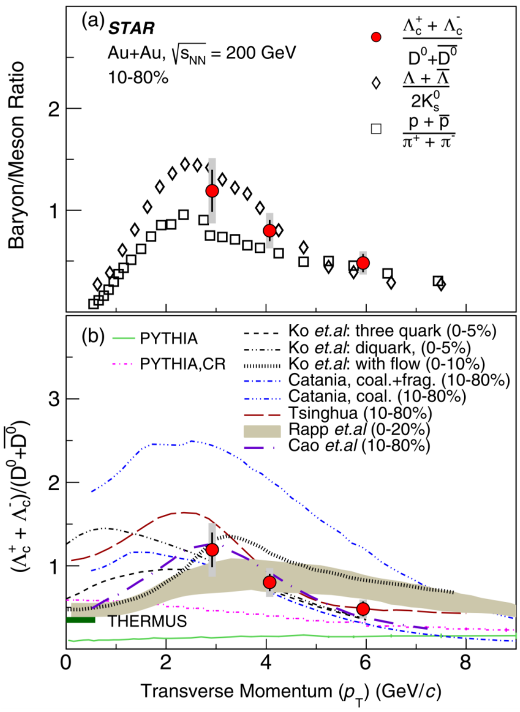

Fig. 7. The $(\Lambda_c^+ + \Lambda_c^-)/(D^0 + \bar{D}^0)$ yield ratio as a function of p_T measured in Au+Au collisions at $\sqrt{s_{NN}} = 200$ GeV by the STAR experiment. The data are compared to (a) baryon-to-meson ratios of strange[30] and light-flavor[31] hadrons and (b) to multiple model calculations.[29,32–35] Figure taken from Ref. 18.

Table 2. Total open charm hadron cross section as measured in 10-40% central Au+Au collisions and in *p*+*p* collisions at 200 GeV.

Collision system	**Hadron**	$d\sigma/dy$ [μb]
Au+Au at 200 GeV Centrality: 10-40%	D^0	41 ± 1 (stat.) ± 5 (sys.)
	$D^\pm$	18 ± 1 (stat.) ± 3 (sys.)
	D_s	15 ± 1 (stat.) ± 5 (sys.)
	Λ_c	78 ± 13 (stat.) ± 28 (sys.)
	Total:	152 ± 13 (stat.) ± 29 (sys.)
p+*p* at 200 GeV	Total:	130 ± 30 (stat.) ± 26 (sys.)

uncertainties. This indicates that the total charm quark production cross section follows the number of binary collision scaling in Au+Au collisions, as expected. On the other hand, the cross sections of individual open-charm hadrons are modified in Au+Au collisions compared to p+p collisions due to the coalescence hadronization of the charm quarks inside the QGP medium which leads to re-distribution of the

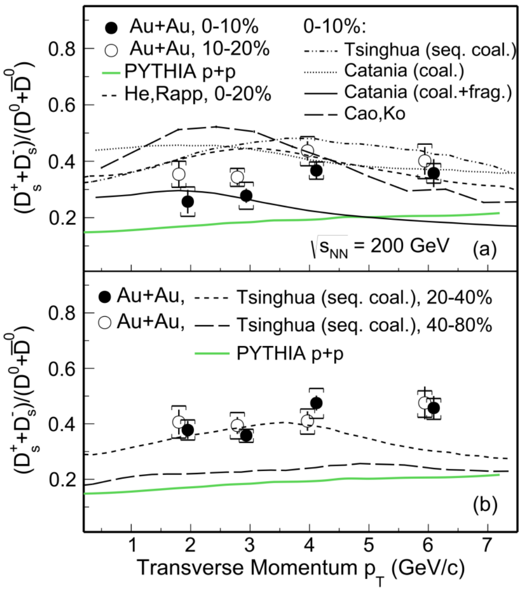

Fig. 8. $(D_s^+ + D_s^-)/(D^0 + \bar{D}^0)$ yield ratio as a function of p_T measured in four different centrality classes of Au+Au collisions at $\sqrt{s_{NN}} = 200\,\text{GeV}$ by the STAR experiment. The data are compared to multiple model calculations.[29,33–35] Figure taken from Ref. 19.

charm quarks among different open-charm hadron species.

3. Summary

The STAR experiment has studied the production of open-charm hadrons in Au+Au collisions in detail. This is possible thanks to the excellent vertex resolution provided by the HFT detector which enables topological reconstruction of hadronic decays of the open-charm hadrons. As a result, STAR has measured invariant yields of D^0, $D^\pm$, $D_s^\pm$ mesons, and Λ_c baryons in Au+Au collisions at $\sqrt{s_{NN}} = 200\,\text{GeV}$.

The D^0 and $D^\pm$ mesons with $p_T > 3\,\text{GeV}/c$ are observed to be suppressed in 0-10% central Au+Au collisions which is consistent with the energy loss of charm quarks inside the QGP medium. The suppression gets smaller going from central to peripheral collisions, which further supports that the modification is due to the presence of the hot and dense medium. The D^0 and $D^\pm$ mesons with $p_T < 3\,\text{GeV}/c$, on the other hand, show significant suppression independent of the collision centrality. This turns out to be important for understanding the charm quark hadronization in heavy-ion collisions. The modification mechanisms are the same for both D^0 and $D^\pm$ mesons, as the $(D^+ + D^-)/(D^0 + \bar{D}^0)$ yield ratio measured in Au+Au collisions is consistent with the PYTHIA calculation within the entire measured p_T range.

In contrast to the D^0 and $D^\pm$ mesons, the Λ_c baryons and $D_s^\pm$ mesons are found to be enhanced with respect to the PYTHA baseline. The measured $(\Lambda_c^+ + \Lambda_c^-)/(D^0 + \bar{D}^0)$ and $(D_s^+ + D_s^-)/(D^0 + \bar{D}^0)$ yield ratios are compared to model calculations incorporating both fragmentation and coalescence hadronization of the charm quarks. Those models describe the data reasonably well, supporting importance of the coalescence hadronization of charm quarks inside the QGP medium at RHIC.

The total charm production cross section per binary nucleon-nucleon collision in Au+Au collisions is consistent with the value measured in p+p collisions, while the QGP causes a re-distribution of the charm quarks among the different open-charm hadron species due to coalescence hadronization of the charm quarks inside the QGP.

Acknowledgements

The work is supported by European Regional Development Fund-Project "Center of Advanced Applied Science" No. CZ.02.1.01/0.0/0.0/16-019/0000778 and by the grant LTT18002 of Ministry of Education, Youth and Sports of the Czech Republic.

References

1. M.M. Aggarwal, *et al.* [WA98 Collaboration], *Eur. Phys. J. C* **23**, 225–236, (2002).
2. D. d'Enterria, *et al.*, *Phys. Lett. B* **19**, 32-43, (2004).
3. A. Adare, *et al.* [PHENIX Collaboration], *Phys. Rev. Lett.* **101**, 232301, (2008).
4. J. Adam, *et al.* [STAR Collaboration], *Phys. Rev. Lett.* **91**, 172302, (2003).
5. K.Aamodt, *et al.* [ALICE Collaboration], *Phys. Lett. B* **696**, 30-39, (2011).
6. S. Chatrchyan, *et al.* [CMS Collaboration], *Eur. Phys. J. C* **72**, 1945, (2012).
7. A. Dainese, C. Loizides and G. Paic, *Eur. Phys. J. C* **38**, 461–474, (2005).
8. I. Vitev and M. Gyulassy, *Phys. Rev. Lett.* **89**, 252301, (2002).
9. I. Vitev, *J Phys G Nucl Part Phys* **30**, S791, (2004).
10. C. A. Salgado and U. A. Wiedemann, *Phys. Rev. D* **68**, 014008, (2003).
11. N. Armesto, A. Dainese, C. A. Salgado, and U. A. Wiedemann, *Phys. Rev. D* **71**, 054027, (2005).
12. T. Renk, H. Holopainen, R. Paatelainen, and K. J. Eskola, *Phys. Rev. C* **84**, 014906, (2011).
13. M. Kliemant, R. Sahoo, T. Schuster, and R. Stock, *et al.*, *Lect. Notes Phys.* **785**, 23-103, (2009).
14. C. Giacomo, *et al.*, *Nucl. Instrum. Methods. Phys. Res. A* **907**, 60-80, (2018).
15. TMVA official website: `http://tmva.sourceforge.net`, (Accessed on: 10/19/2021).
16. M. Tanabashi, *et al.*, *Phys. Rev. D* **98**, 030001, (2018).
17. Adam, J., *et al.* [STAR Collaboration], *Phys. Rev. C* **99**, 034908, (2019).
18. Adam, J., *et al.* [STAR Collaboration], *Phys. Rev. Lett.* **124**, 172301, (2020).
19. Adam, J., *et al.* [STAR Collaboration], *Phys. Rev. Lett.* **127**, 092301, (2021).
20. Abelev, B.I., *et al.* [STAR Collaboration], *Phys. Lett. B* **655**, 104, (2007).
21. Cao, S., Luo, T., Qin, G. Y., and Wang, X. N., *Phys. Rev. C* **94**, 014909, (2016).
22. Xu, Y., Bernhard, J. E., Bass, S. A., Nahrgang, M., and Cao, S., *Phys. Rev. C* **97**, 014907, (2018).
23. Abelev, B.I., *et al.* [STAR Collaboration], *Phys. Lett. B* **655**, 104, (2007).

24. Abelev, B.I., *et al.* [ALICE Collaboration], *Phys. Lett. B* **720**, 52, (2013). 720, 52 (2013).
25. Adam, J., *et al.* [ALICE Collaboration], *J. High Energ. Phys.* **2016**, 81, (2016).
26. Adamczyk, L., *et al.* [STAR Collaboration], *Phys. Rev. D* **86**, 072013, (2012).
27. Adamczyk, L., *et al.* [STAR Collaboration], *Phys. Rev. Lett.* **113**, 142301, (2014); **121**, 229901, (2018).
28. Trotbjörn, S., *et al.*, *Comput. Phys. Commun.* **191**, 159-177, (2015).
29. S. Plumari, V. Minissale, S. K. Das, G. Coci and V. Greco, *Eur. Phys. J. C* **78**, 348, (2018).
30. Agakishiev, G., *et al.* [STAR Collaboration], *Phys. Rev. Lett.* **108**, 072301, (2012).
31. Abelev, B.I., *et al.* [STAR Collaboration], *Phys. Rev. Lett.* **97**, 152301, (2006).
32. Cho, S., Sun, K.-J., Ko, Ch. M., Lee, S. H., and Oh, Y., *Phys. Rev. C* **101**, 024909 , (2020).
33. Zhao J., Shi, S., Xu, N., Zhuang, P., arXiv:1805.10858v1
34. He, M. and Rapp, R., *Phys. Rev. Lett.* **124**, 042301, (2020).
35. Cao, S., *et al.*, *Phys. Lett. B* **807**, 135561, (2020).